THE FLORIDA STATE UNIVERSITY

COLLEGE OF ARTS AND SCIENCES

NORTH ATLANTIC AND NORTHEAST PACIFIC TROPICAL CYCLONE INTENSITY COMPARISON USING INTEGRATED KINETIC ENERGY

By

JACOB CARSTENS

A Thesis submitted to the
Department of Earth, Ocean, and Atmospheric Science
in partial fulfillment of the requirements for graduation with Honors in the Major

Degree Awarded: Spring, 2017.

The members of the Defense Committee approve the thesis of Jacob Carstens defended on March 31, 2017.

Thesis Director: _____ Date: _____

2nd Committee Member: _____ Date: _____

Outside Committee Member: _____ Date: _____

Abstract

The Integrated Kinetic Energy (IKE) of tropical cyclones (TCs) in the Northeast Pacific (NEP) basin is computed from the Extended Best Track Dataset from 2004-2013. Analysis of extreme terciles is conducted based on the IKE values of the TCs and compared with those of the North Atlantic (AL) basin. Analysis reveals that large (small) IKE TCs in the NEP basin are generally in the open waters (closer to coast), have their genesis closer to the equator (more latitudinal diversity), have a more zonal motion of TC (meridional component of motion is significant), and prevalent in the later part of the season (no preferred time of the season). The comparison with the TCs of the AL basin reveals qualitatively similar characteristics of the extreme terciles based on their IKE values. However, there are salient differences in the IKE characteristics of TCs between the two basins, which are highlighted by the contrast in the rainfall volumes within the gale strength wind radii of the TCs. The TCs of the NEP basin carry much lower rainfall volumes than their AL counterparts, in addition to generally having lower IKE. Furthermore, we have developed a linear regression equation to predict the rainfall volume of the TC from its IKE value. This equation tends to predict rainfall volume reasonably well from IKE in a perfect prognostic approach, with some subtle differences in its performance between the two basins.

1. INTRODUCTION

In recent years, the North Atlantic Tropical Cyclone (TC) basin has produced several highly destructive TCs that were not considered particularly intense on the Saffir-Simpson intensity scale. Sandy (2012) is the most profound example, causing an estimated $75 billion in damage despite peaking at only Category 3 intensity. These TCs have led to reasonable doubt on the use of maximum wind speed as a comprehensive measurement of intensity (Powell and Reinhold 2007; Yu et al. 2012; Misra et al. 2013). Powell and Reinhold (2007) set out to provide a more complete description of TC intensity by accounting for the entire tropical storm-force wind field around the center of the TC. In the study, they argue that tropical storm-force winds and stronger cause the greatest damage in landfalling TCs due to both wind energy and storm surge-induced flooding. Integrated Kinetic Energy (IKE) was the result, representing the kinetic energy of the TC's entire wind field inside an enclosed radius of 34+ knot wind.

The IKE concept has expanded over the last decade. Misra et al. (2014) analyzed accumulated IKE over the lifespan of the TC and season, known as Track Integrated Kinetic Energy (TIKE). Here, studies were performed regarding IKE climatology from 1990-2011, as well as analyses of TIKE's relation to SST distributions. Following this, Statistical Prediction of Integrated Kinetic Energy (SPIKE; Kozar and Misra 2015; Kozar 2016) was developed to predict IKE up to 72 hours out, often outperforming IKE forecasts produced via NHC wind radii projections. However, all prior research involving IKE has only concerned the North Atlantic (AL) basin. The concept was not ready to be applied to other basins, simply because aircraft reconnaissance data was either unavailable or too inconsistent. IKE relies on estimates of 34, 50, and 64 knot wind radii provided by the Cooperative Institute for Research in the Atmosphere

(CIRA) at Colorado State University (Demuth et al. 2004), whose coverage is not uniform in the other tropical basins (i.e. the data are sporadic and does not cover most TC fixes), and was unavailable in the Northeast Pacific (NEP) basin until 2001.

We now have higher quality NHC estimates (best tracked) for ten NEP seasons (2004-2013; http://www.nhc.noaa.gov/data/hurdat/hurdat2-format-nencpac.pdf), in addition to their AL counterparts (http://www.nhc.noaa.gov/data/hurdat/hurdat2-format-atlantic.pdf). Thus, we have the means to compute and analyze IKE for these NEP TCs, and can perform comparisons between the AL and NEP basins from 2004-2013. Five sections will follow in this paper: Review of research relevant to the task at hand, datasets used in the study, methodology, results, and associated conclusions. The specific objectives of this project are:

1. Compare the IKE of TCs in the NEP and AL basins. This will be accomplished by comparing the distribution of IKE in seasonal climatology, composite analysis based on extreme terciles, and scatter plots and linear regression fits involving IKE. IKE will be examined in relation to TC genesis location and track, rainfall volume, and rainfall distribution. From this, we aim to diagnose particular regions and paths that favor intensification (defined in this study as increases in IKE rather than maximum wind speed).
2. Discern the relationship of rainfall volume (RV) with the size of the TC, as well as its distribution within the TC's wind field. A particular goal of this study is to diagnose the relationship between IKE and RV, and develop a forecasting methodology for total TC rainfall based on projections of IKE. This particular study will invoke the use of a simple

linear regression forecast model, with a plan to utilize more complex statistical techniques such as the artificial neural network in future studies.

2. REVIEW OF RELEVANT PRIOR WORK

A notable flaw in the use of maximum wind speed as the definition of TC intensity is the uncertainty that exists in its estimation, as measurements by aircraft reconnaissance flights are error-prone (Hock and Franklin 1999; Franklin et al. 2003). While the NHC officially estimates maximum winds to be marginally higher than recon data suggests, confusion still exists as to what these maxima are (Nolan et al. 2014). To examine this issue, Uhlhorn and Nolan (2012) simulated 2003's Hurricane Isabel using a numerical model and archived aircraft data from the time of the hurricane. Using the model's generation of wind speeds near the center, aircraft data had 7-10% underestimation errors for the 1-minute sustained wind speed. This inaccuracy provides insight to the importance of examining alternative metrics for TC intensity, such as IKE.

Wind radius accuracy is the backbone of effective IKE computation, so critical to this research is the accuracy of aircraft, satellite, and buoy data for both wind speed and distance from the center of a TC. The NHC has performed forecasts of hurricane force (64 knot) winds up to 36 hours, as well as damaging (50) and gale (34) force up to 72 hours, since 2004. With the help of model guidance beginning in 2005, forecasting has improved, with errors reducing from

40% to 24% for 24-hour forecasts from 2004-2013, and the most substantial improvement occurring from 2010-2013 (Knaff and Sampson 2015).

The work of Chavas and Emanuel (2010) can help us in developing hypotheses on numerical IKE comparisons between the NEP and AL. They used satellite data records from 1999-2008 to analyze the average size of TCs in each tropical ocean basin. To accomplish this, they employed an outer wind model, which assumed no deep convection, to provide an estimation of the maximum radial extent of the TC by diagnosing the zero-wind radius. They showed that the NEP storms had the smallest average radial extent, roughly 341 km compared to the global median of 423 km. This preliminarily study suggests that AL TCs would have higher IKE and a more widely spread destructive potential compared to the NEP TCs, based on size alone. Knaff et al. (2014) expanded this analysis of storm size to include a 34-season climatology based on infrared imagery accumulated from 1978-2011. Their results further supported the observation that NEP TCs were generally smaller, and concluded that no long-term changes existed for TC size due to climate change. Finally, they found that smaller (larger) TCs tended to be westward (northward) steering and located at lower latitudes in the NEP.

A comprehensive study was performed by Cerveny and Newman (2000) to diagnose the relationship between TC intensity and precipitation across the AL, NEP, and West Pacific basins. They used satellite-derived precipitation records from 1979-1995, accounting for 877 total TCs and 5775 daily precipitation observations. There existed a robust relationship between wind speed and daily rainfall accumulation. Data was split between an inner core within the TC's region of peak intensity, and a comprehensive outer section encompassing the TC's full radial

extent. The distribution of inner core rainfall followed a parabolic pattern, with the highest percentages of inner core rain coming in weak tropical storms and major hurricanes (roughly 35%). A lower inner core rain percentage (25%) in the middle of the intensity range suggests that rainfall and flooding potential may be more widely distributed in TCs of moderate intensity (Figure 1). A regression equation was also generated, which suggests that for each 10 knot increase in maximum wind speed, the daily precipitation increases by about 13 mm. We are alternatively attempting in this study to determine the relationships between IKE and TC rainfall in both the AL and NEP.

3. DATA

Two primary datasets are used in this project. The first is the Extended Best Track (EBT) Dataset from Colorado State University [Available at: http://rammb.cira.colostate.edu/research/tropical_cyclones/tc_extended_best_track_dataset/], which combines NHC observations with postseason re-analysis that attempts to depict TC structure, including but not limited to: radii of 34, 50, and 64 knot winds, radius and pressure of the outermost closed isobar, and latitude, longitude, and pressure at the TC's center. This data exists at intervals of 6 hours over the lifespans of TCs that reached at least tropical storm status.

Though NEP data extends back to 2001 and AL to 1988, this study begins with the 2004 season, which is when the NHC began to perform postseason reanalysis of the necessary wind radii values (best tracked). Prior to 2004, this was done by more error-prone operational estimation at the time of the TC. 143 TCs (2169 fixes) developed in the NEP during this period,

and 161 (2882) in the AL. IKE data is split into two separate groups of terciles for each basin. One encompasses the entire set of IKE values, while the other only considers the maximum value of IKE achieved by each TC. In the track analyses, the upper and lower terciles for each basin are compared with one another. The smaller set of terciles using maximum IKE included 48 TCs in the NEP, and 54 in the AL, while the larger comprehensive set included 723 TC fixes in the NEP, and 961 in the AL.

The second dataset is the Tropical Rainfall Measuring Mission (TRMM) 3B42, a 3-hourly rainfall rate dataset at a 0.25° grid spacing from NASA, extending from 1 January 1998 to the present day (Huffman et al. 1995). This only measures rainfall up to latitudes of 49.875° in both hemispheres (just north of the United States-Canada border, but by this time TCs often reach extratropical status and are thus no longer considered for IKE computation). This is used to compute the rainfall volume within each TC at the 6-hourly fixes from the Extended Best Track set, as the dataset measures rainfall rate in mm hr^{-1}. Computational strategy will be outlined in the next section.

4. METHODOLOGY

IKE is computed (following Powell and Reinhold 2007) using the wind speed and radii data from the EBT Dataset. The equation for IKE is as follows:

$$IKE = \int_V \frac{1}{2}\rho U^2 dV \quad \text{----------(1)}$$

where ρ is the air density approximated as a constant at 1 kg m^{-3}, U is the 10-m wind speed in m/s, and the volume integral is computed at a depth of 1-m centered at the 10-m level, encompassing the area where winds exceed tropical storm strength (34 knots or 18 m/s). IKE is calculated for each TC at six hour intervals for which the TC has maximum sustained winds of 34 knots or greater, if operational or post-storm data are available. It should also be noted that IKE is designed as an indicator of a storm's destructive potential (Powell and Reinhold 2007), and therefore does not account for wind speeds below tropical storm strength.

The formulae to calculate IKE from the wind radii data were originally published by Powell and Reinhold (2007), based on radii from the HWind analysis product (Powell et al. 1998). However, wind radii tend to be slightly overestimated in HWind analysis (Moyer et al. 2007), so it is appropriate to utilize the altered formulae as described by Powell (2008) and Misra et al. (2013). These use Equation (1) but with the conditions listed in Table 1. Kinetic energy is calculated by using an estimation of the mean wind between each quadrant wind radius, where 34, 50, and 64 kt winds are the threshold values. The kinetic energy is then integrated over the area to obtain IKE.

Locational analysis is performed from the composites (described above) using the latitude and longitude of the TC's center at any given fix and assigning (or binning) it to a 1º x 1º grid cell. We accumulate the number of TCs for each type of composite that are within this grid cell across the 2004-2013 timespan. The result of this accumulation is the density plot which we produce for the upper and lower IKE terciles in each basin.

We also computed the rainfall volume (RV) for each TC fix in both basins as:

$$RV = \int_0^{r_{XX}} Rdr \quad (2)$$

where, r_{XX} is the specified wind radii from the center of the TC fix and R is the rain rate. We also computed RV within specific wind radii bands of the TC (e.g., 34-50kt, 50-64kt, >64kt). For the gridded TRMM-3B42 rainfall dataset at 0.25° x 0.25° spatial resolution, equation 2 takes the discrete form of:

$$RV = \sum_{i=1}^{N} R_i A_i \quad (3)$$

where, N is the total number of grid points within the radius r_{xx} of each quadrant of the TC and A_i is area of the grid box.

5. RESULTS

IKE COMPUTATION/CLIMATOLOGY

The first computations of NEP IKE have been performed in this study, as well as expansion of the AL IKE database to include the 2012 and 2013 seasons. As expected, due to the generally smaller size of NEP TCs, IKE is on average much lower here than in the AL (Figure 2). An example is the maximum IKE for each basin, which was 122.26 TJ in the NEP (Hilary 2005), compared to 433.90 TJ for the AL (Sandy 2012). The upper tercile thresholds for maximum IKE per individual TC were 37.13 TJ (AL) versus 17.84 TJ (NEP). Hurricane Hilary

in 2005 is the only TC in the NEP storm to exceed 100 TJ of IKE at any point, while 24 TCs in the same period attained this in the AL.

Monthly averages for both instantaneous IKE and TC count are included in Figure 3. In both basins, IKE peaks in September, generally considered the seasonal peak under the current definition of intensity. This peak is more pronounced in the AL, with an average single-fix IKE of nearly 40 TJ. This is especially noteworthy given the presence of Sandy and Wilma in this dataset, which both occurred in October. Sandy attained the highest IKE in the 1990-2013 database, peaking at over 430 TJ, while Wilma was one of the most intense AL hurricanes ever under the current definition, attaining the sixth highest peak IKE from 2004-2013. Our NEP climatology also reflects the current standard, with a peak in TC count in August, and average IKE just lower than September's peak of ~12 TJ.

Of note is the lack of significant drop-off in average IKE at the end of the AL season. Sandy again serves a strong example of the reasoning for this, as late-season TCs that approach the United States coast tend to curve northward, because of both the northward increase in Coriolis acceleration and influence of westerly steering flow at higher latitudes, and undergo extratropical transition. This will weaken the TC under current intensity definitions, as the TC enters regions of cooler waters and higher vertical wind shear on average, but significant horizontal expansion is also a typical consequence. Because IKE is more dependent on TC size than maximum wind, the net effect is a sharp increase in IKE, as was seen in Sandy's rise to the top of the IKE scale.

TC TRACK/LOCATIONAL IMPACT ON IKE

A. GENESIS

Here, we define genesis as the first location at which IKE is measured for each TC. As a reminder, our tercile system here is based on the maximum IKE attained by each TC. As displayed in Figure 4, for both basins, TCs in the lower IKE terciles showed less concentration, with much more spread across the map and a northerly shift in average genesis location compared to the upper terciles. In the NEP, the northerly shift is more obvious, as no TCs in its upper tercile have genesis north of 18°N, compared to 6 in the lower tercile. Less intense TCs also tend to concentrate closer to the Mexican coast, an expected correlation given the negative impact of landmasses on TC intensity due to cutoff of latent heat production. For the AL, the key trend is a heavy concentration of upper tercile TCs in the open waters near Africa, a typical starting point for many intense late-season hurricanes, with a much more disorganized distribution pattern in the lower tercile.

B. MAXIMUM IKE

In the NEP, we see an influence of track on IKE intensification. As Figure 5 showcases, TCs in the lower tercile tend to track along the Mexican coast and achieve maximum IKE further to the north and east, as compared to TCs in the upper tercile. Stronger TCs maximize over the open Pacific waters between Mexico and Hawaii and tend to concentrate at lower latitudes. The North Atlantic showcases a pronounced northerly trend, as TCs tend to expand in their turn away from the United States coast and

the associated transition to extratropical status. As was discussed in the previous section, wind radii increase to compensate for the likely decrease in maximum wind speed, leading to these higher IKE values given a lack of landmass interaction. Another focal point is in the Gulf of Mexico, a region primarily consisting of TCs which avoided the topography of the Caribbean islands. On the contrary, there is a heavy concentration of less intense TCs in the Caribbean; largely those that made landfall over these islands and lost its organization.

C. COMPREHENSIVE IKE DISTRIBUTION

These are much more expansive plots, encompassing one third of all IKE totals for the respective basins per plot. As Figure 6 demonstrates, the strongest concentrations of high IKE values in the AL tend to occur along two bands, the first being the open waters of the Caribbean Sea into the Gulf of Mexico, and the second running just north of the Caribbean islands towards the U.S. east coast. Many of the higher IKE values in the NEP occur along a band extending from 12°N to 20°N, with more variability in the lower terciles for both basins and a higher tendency to track towards land, as is expected.

RAINFALL VOLUME COMPUTATION AND FORECASTING

Aligning with expectation, RV values in the AL tend to be much higher than those in the NEP. The average RV per TC fix at 2.476 km^3 in the AL, compared to 0.952 km^3 in the NEP. We also accumulated the total rainfall volume over the entire season in each basin, which on

average was roughly 700 km^3 in the AL compared to 198 km^3 in the NEP. A full list of comparisons, including the average TC-accumulated rainfall volume, is available in Table 1. From here, we discerned the relationships between these RV values and storm size, using the median radii of 34, 50, and 64 knot winds available from the Extended Best Track dataset. Relatively strong positive correlations exist in all cases, though sample size decreases as we approach the 64 knot cases (as we are only to use the hurricane-force fixes within the set). In both basins, the strongest correlation exists between RV and 50 knot wind radii (both strong tropical storms and hurricanes included), with R^2 settling in the 0.7-0.75 range (full listing of these coefficients provided in the figures below).

As a preliminary foray into using IKE to forecast total TC rainfall, we recap our linear regression forecast methodology. Given a 10-year dataset for each basin, we use IKE and RV data from 2004-2011 to build separate simple linear regression equations for each basin that express RV as a function of IKE. With the remaining IKE data currently accounted for from the 2012 and 2013 seasons, we use the generated regression equation to predict RV at each TC fix. We then compare the predicted value to RV to the actual value computed previously, representing our forecast error.

Table 2 highlights the relatively strong linear relationship of IKE and RV for TCs in both ocean basins from a simple linear regression fit to the scatter shown in Fig. 6. It is observed that the R^2 between IKE and RV for AL TCs is 0.64 and that for the NEP is 0.44. The distribution of rainfall within the TC proves to have much higher variability. Using the subset of hurricane-strength fixes, we determined that the outer extent of the storm (area between the 34 and 50 knot

wind radii) contributed about 75% of the total TC rainfall on average, though for individual TCs, the contribution was as low as 21% (Figure 8). Table 2 also provides the corresponding RMS error (RMSE) of the linear fit, which is given by:

$$RMSE = \sqrt{\frac{1}{N}\sum_{i=1}^{N}\left[A_i - \hat{A}_i\right]^2} \quad (4)$$

where, A_i and $\hat{A}_i$ are the observed and estimated RV for a given TC fix (i). The RMSE values in Table 2 are 1.64 km^3 and 0.76 km^3 that correspond to ~ 66% and 80% of the average observed RV per TC fix for the AL and NEP basins respectively. Most NEP RV forecasts are accurate to within 1 km^3, though a tendency for underestimation begins as IKE increases. In the AL, larger TCs and an inherent larger IKE range create more error across the RV forecast spectrum (Figure 9). Sandy is included in the forecast dataset here, and the regression equation grossly overestimated its rainfall upon exceeding 200 TJ of IKE. The following general trend is observed across both basins: forecast quality is higher at lower values of IKE.

6. CONCLUSIONS

In this study, we have compared the TCs of the Northeast Pacific (NEP) and the North Atlantic (AL) basins based on their Integrated Kinetic Energy (IKE) characteristics. IKE is significantly affected by the size and the wind distribution around the azimuth of the TC. We find that TC's of the NEP basin have invariably much lower IKE than those in the Atlantic. This stems from the fact that TC in the AL basin span a much larger longitude band and also have a tendency to recurve into higher latitudes, where they tend to acquire larger size from extra-

tropical transition. Therefore, the differences in IKE between TCs of AL and NEP are larger in the later part of the hurricane season, when a significant number of TCs in AL have a tendency to propagate to higher latitudes.

The composite analysis reveals that TCs with larger IKE in both basins have more of a deep tropical origin. However, because of a larger longitudinal span of genesis for AL TCs, the genesis density of large IKE TCs are weaker than for the NEP large IKE TCs. In the NEP basin, the TCs with lower maximum IKE are further north and east (more along the Mexican coast) than the TCs with higher maximum IKE that are further west (in the open waters) and typically south of 16°N. In the Atlantic, for TC's with lower maximum IKE we observe a larger spread of TC locations from the eastern Atlantic (e.g. Cape Verde type TCs) to those over the Caribbean Sea and the Gulf of Mexico, where TCs are likely to spend less time over the waters for it to further intensify. However, the figure suggests there are also comparable small sized TCs forming in the subtropical latitudes of the AL basin. The AL TCs with higher maximum IKE show clear preference of location in the northern latitudes, where by extra-tropical transition they can acquire larger size.

In the AL basin, the higher IKE TCs have more northward track while the lower IKE TCs have a more zonal track. Further, the lower latitude origins of the tracks are more prominent for the lower IKE than the higher IKE TCs in the Atlantic. In contrast, in the NEP basin the tracks of the TCs with higher IKE are more zonally oriented and extend further westward than for the TCs with lower IKE. Further, the tracks of TCs in the NEP are confined to a narrower latitude band for TCs with higher IKE than those with lower IKE.

Rainfall volume (RV) is computed as the volume integral up to the wind radii of tropical storm strength for each available quadrant at each TC fix. This estimate of RV of a TC should represent a good fraction of the total rain of the TC following the observational study of Cerveny and Newman (2000) who noted that the rainfall in the inner core of the TC is a good representation of the total rainfall from the TC. It is found that the RV for NEP TCs are far less than for the AL TCs. For example, the average RV per TC fix is 2.476 km^3 for the AL basin compared to 0.952 km^3 for the NEP basin. Further, the accumulated total RV over the entire season in each basin was ~700 km^3 in the Atlantic compared to 198 km^3 in the NEP.

A simple linear regression model relating RV to IKE of the TC was developed for each basin and tested in a perfect prognosis approach. The performance of this model in a cross-validation sense revealed that it is able capture the RV for small IKE TCs far better than the larger sized TCs in both basins. However, in the AL basin this model systematically overestimates the RV for larger sized TCs. In the NEP, it tends to both over and under estimate RV in the samples of large sized TCs. This is likely because the large sized TCs in the AL are invariably at higher latitudes compared to those in the NEP. And as Cerveny and Newman (2000) note, TCs display a large latitudinal gradient in rainfall in both these basins with a larger fraction of TC rainfall occurring in the deep tropics, which coincides with the higher moisture availability in the tropical atmospheric column.

REFERENCES

Cerveny, R.S. and L.E. Newman, 2000: Climatological relationships between tropical cyclones and rainfall. *Mon. Wea. Rev.*, **128**, 3329–3336. [Available online at: http://journals.ametsoc.org/doi/pdf/10.1175/1520-0493(2000)128%3C3329:CRBTCA%3E2.0.CO;2]

Chavas, D.R. and K.A. Emanuel, 2010: A QuikSCAT climatology of tropical cyclone size *Geophysical Research Letters*, **37**, L18816, doi: 10.1029/2010GL044558

Demuth, J.L, M. DeMaria, J.A. Knaff, and T.H. Vonder Haar, 2003: Evaluation of Advanced Microwave Sounding Unit tropical-cyclone intensity and size estimation algorithms. *J. Appl. Meteor.*, **43**, 282–296, doi: 10.1175/15200450(2004)043<0282:EOAMSU>2.0.CO;2

Donlon, C. J., M. Martin, J. D. Stark, J. Roberts-Jones, E. Fiedler and W. Wimmer, 2011. The Operational Sea Surface Temperature and Sea Ice analysis (OSTIA). *Remote Sensing of the Environment.* doi: 10.1016/j.rse.2010.10.017 2011.

Franklin, J. L., M. L. Black, and K. Valde, 2003: GPS dropwindsonde profiles in hurricanes and their operational implications. *Wea. Forecasting*, **18**, 32–44, doi: 10.1175/1520-0434(2003)018,0032: GDWPIH.2.0.CO;2.

Hock, T. F., and J. L. Franklin, 1999: The NCAR GPS dropsonde. *Bull. Amer. Meteor. Soc*., **80**, 407–420, doi: 10.1175/ 1520-0477(1999)080,0407:TNGD.2.0.CO;2.

Huffman, G.J., R. F. Adler, B. Rudolf, U. Schneider, and P. R. Keehn, 1995: Global precipitation estimates based on a technique for combining satellite-based estimates, rain gauge analysis, and NWP model precipitation information. *J. Climate,* **8,** 1284–1295.

Knaff, J.A., S.P. Longmore, and D.A. Molenar, 2014: An objective satellite-based tropical cyclone size climatology. *J. Climate*, **27**, 455–476, doi: 10.1175/JCLI-D-13-00096.1

Knaff, J.A. and C.R. Sampson, 2015: After a decade are Atlantic tropical cyclone gale force wind radii forecasts now skillful? *Wea. Forecasting*, **30**, 702–709, doi: 10.1175/WAF-D-14-00149.1

Kozar, M.E. and V. Misra, 2014: Statistical prediction of integrated kinetic energy in North Atlantic tropical cyclones. *Mon. Wea. Rev.*, **142**, 4646–4657, doi: 10.1175/MWR-D-14-00117.1

Misra, V., S. DiNapoli, and M. Powell, 2013: The track integrated kinetic energy of Atlantic tropical cyclones. *Mon. Wea. Rev.*, **141**, 2383–2389, doi: 10.1175/MWR-D-12-00349.1

Nolan, David S., Jun A. Zhang, and Eric. W. Uhlhorn, 2014: On the limits of estimating the maximum wind speeds in hurricanes. Mon. Wea. *Rev*., **142**, 2814–2837.

Moyer, A. C., J. L. Evans, and M. Powell, 2007: Comparison of observed gale radius statistics. *Meteorol. Atmos. Phys.*, **97**, 41–55.

Powell, M.D. and T.A. Reinhold, 2007: Tropical cyclone destructive potential by integrated kinetic energy. *Bull. Amer. Met. Soc.,* **88**, 513–526, doi: 10.1175/BAMS-88-4-513

Powell, M.D. and E.W. Uhlhorn, 2009: Estimating maximum surface winds from hurricane reconnaissance measurements. *Wea. Forecasting*, **24**, 868–883, doi: 10.1175/2008WAF2007087.1

Rienecker, M.M., et al., 2011: MERRA: NASA's Modern-Era Retrospective Analysis for Research and Applications. *J. Climate*, **24**, 3624–3648, doi: 10.1175/JCLI-D-11-00015.1

Suarez, M. and Bacmeister, J., 2015: Development of the GEOS-5 atmospheric general circulation model: evolution from MERRA to MERRA2, Geosci. Model Dev., **8**, 1339–1356, doi: 10.5194/gmd-8-1339-2015.

Uhlhorn, E.W. and D.S. Nolan, 2012: Observational undersampling in tropical cyclones and implications for estimated intensity. *Mon. Wea. Rev.*, **140**, 825–840, doi: 10.1175/MWR-D-11-00073.1

Yu, J.-Y., and P.-G. Chiu, 2012: Contrasting various metrics for measuring tropical cyclone activity. Terr. Atmos. Oceanic Sci., **23**, 303–316.

TABLES

TABLE 1: Guidelines for computing IKE based on 34, 50, and 64 knot wind radii. (Borrowed from Misra et al. 2013)

Quadrant IKE contribution	Criteria	Mean wind ($m\,s^{-1}$)	Area (m^2)
IKE_{18-26}	$R_{26} > 0$	20	$0.25\pi(R_{18}^2 - R_{26}^2)$
	No R_{26}, $V_{MS} > 26$, $R_{18} > R_{max}$	20	$0.25\pi[R_{18}^2 - (0.75R_{max})^2]$
	No R_{26}, $V_{MS} < 26$, $R_{18} > R_{max}$	$0.25V_{MS} + 0.75(18)$	$0.25\pi[R_{18}^2 - (0.75R_{max})^2]$
	No R_{26}, $R_{max} = R_{18}$	18	$0.25\pi[R_{18}^2 - (0.5R_{18})^2]$
IKE_{26-33}	$R_{33} > 0$	27.75	$0.25\pi(R_{26}^2 - R_{33}^2)$
	No R_{33}, $V_{MS} > 33$, $R_{26} > R_{max}$	27.75	$0.25\pi[R_{26}^2 - (0.75R_{max})^2]$
	No R_{33}, $V_{MS} < 33$, $R_{26} > R_{max}$	$0.25V_{MS} + 0.75(26)$	$0.25\pi[R_{26}^2 - (0.75R_{max})^2]$
	No R_{33}, $R_{26} \le R_{max}$	26	$0.25\pi[R_{26}^2 - (0.5R_{26})^2]$
IKE_H	Max R_{33} quadrant, $R_{33} > R_{max}$	$0.25V_{MS} + 0.75(33)$	$0.25\pi[R_{33}^2 - (0.75R_{max})^2]$
	Max R_{33} quadrant, $R_{33} = R_{max}$	$0.25V_{MS} + 0.75(33)$	$0.25\pi[R_{33}^2 - (0.75R_{33})^2]$
	$R_{33} < R_{max}$	$0.1V_{MS} + 0.9(33)$	$0.25\pi[R_{33}^2 - (0.75R_{33})^2]$
	Not max R_{33} quadrant, $R_{max} = R_{33}$	$0.1V_{MS} + 0.9(33)$	$0.25\pi[R_{33}^2 - (0.75R_{max})^2]$

TABLE 2: Average rainfall volume statistical comparison between the North Atlantic and East Pacific basins, based on both instantaneous and accumulated TC rainfall.

(All values are in km^3)	**North Atlantic**	**East Pacific**
Average individual fix RV	2.47612	0.951605
Average total storm RV	43.5671	13.8573
Average seasonal RV	701.430	198.160
Max individual fix RV	~25	~9

TABLE 3: Correlation statistics between IKE and rainfall volume for the North Atlantic and East Pacific basins.

	North Atlantic	**East Pacific**
RV/IKE R^2	0.6412	0.4440
RMS Error (km^3)	0.6537	0.2161
Regression Equation	RV = 0.79 + 0.0596(IKE)	RV = 0.32 + 0.0589(IKE)

FIGURES

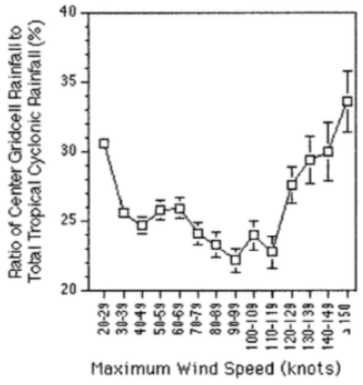

Figure 1: Relationship between maximum wind speed of a TC and the distribution of its rainfall near its center. Note the general parabolic pattern here, indicating a potential relationship between our varying IKE ranges and their associated rainfall distributions that may mirror this (Borrowed from Cerveny and Newman 2000).

Commented [MB1]: What is meant by the error bars? That should be in the caption'

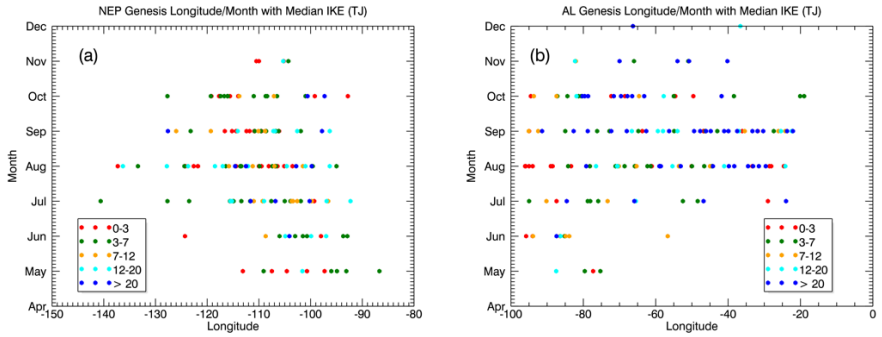

Figure 2: The month and longitude of genesis for a) East Pacific and b) North Atlantic TCs, split into five categories based on the median IKE value each storm had during its lifespan.

Commented [MB2]: Explain the colors – what specifically do they represent

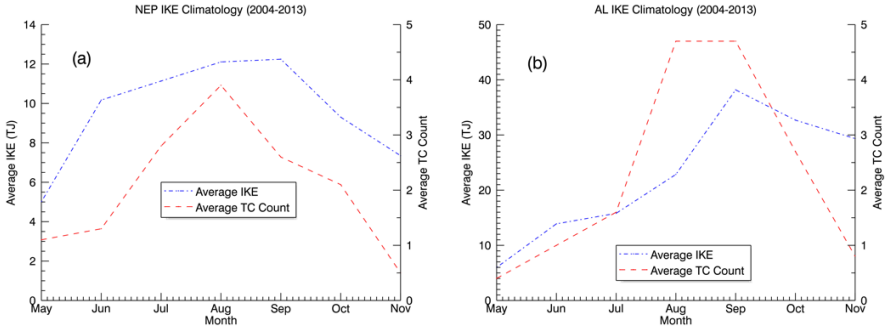

Figure 3: Climatology of IKE over the 10-year dataset for the a) East Pacific and b) North Atlantic basins. The blue line represents the average instantaneous IKE value per month; the red line indicates the average number of TCs that develop per month. Scaling is different in the North Atlantic plot to reflect the larger average IKE throughout the season.

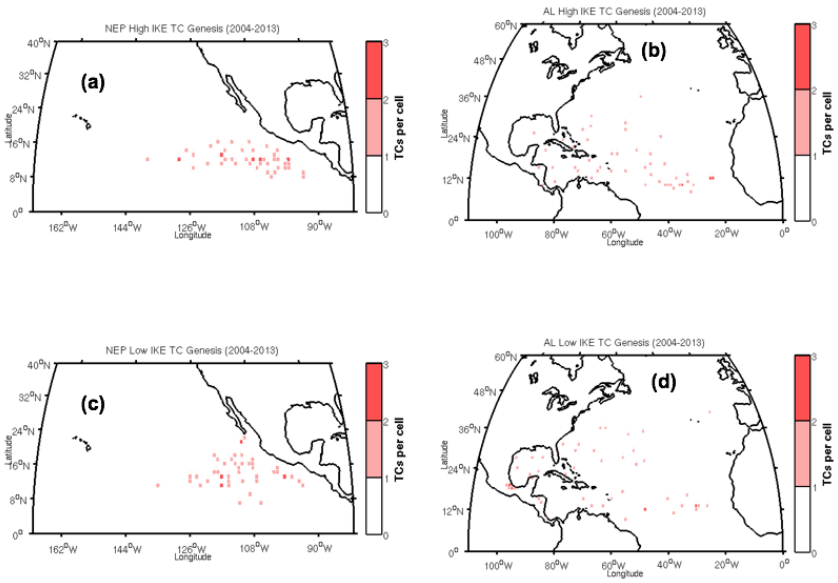

Figure 4: Storm genesis plots for the upper and lower terciles of each of the study's two TC basins. The terciles are determined according to the maximum IKE achieved by each individual storm. Density is plotted according to the location of the storm's center at the time of its first IKE computation, with 1° grid spacing on the cells.

Commented [MB3]: There is no way these are terciles unless key information is missing (i.e., a statement of what each figure represents, and what is meant by white in the color bar).

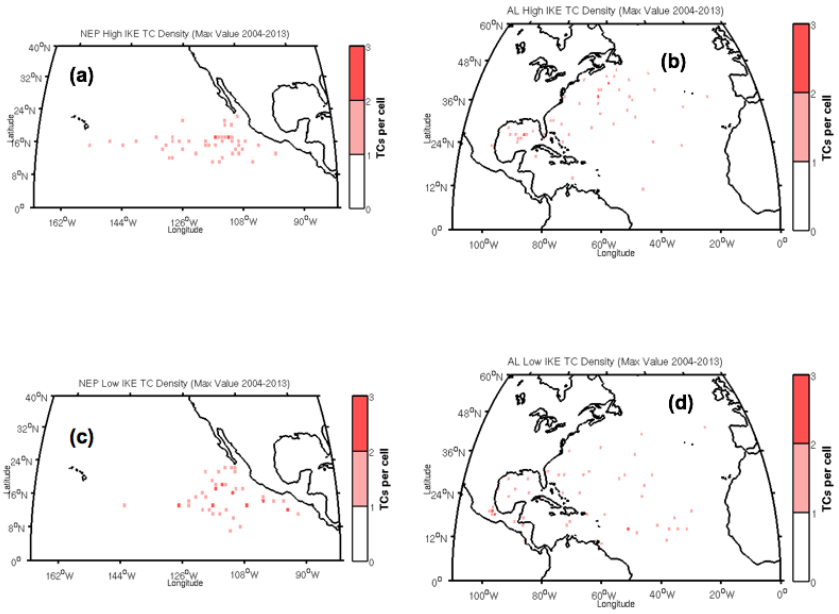

Figure 5: Maximum IKE density plots for the upper and lower terciles in each basin. Here, densities are plotted based on the location of the storm's center at the time of its maximum IKE value, using the same grid spacing rules as in Fig. 2. Fig. 4 will also follow these guidelines.

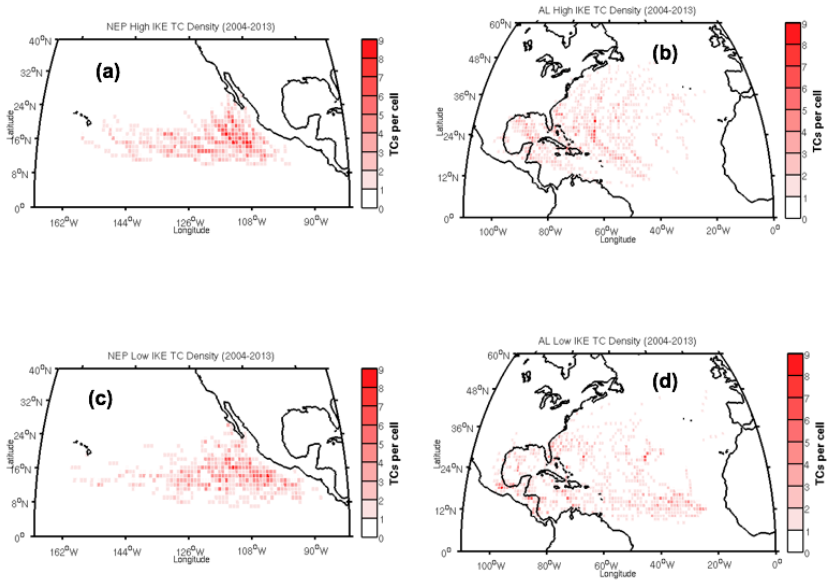

Figure 6: Comprehensive IKE track density plots for each basin. Here, all IKE values over the 2004-2013 seasons are split into upper and lower terciles, and plotted using the same grid spacing rules as in the previous two figures.

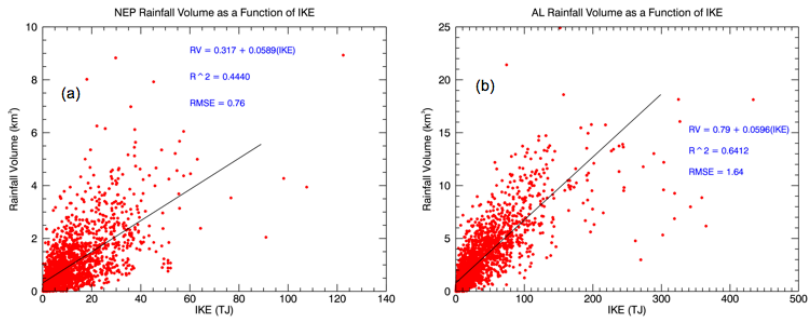

Figure 7: Scatterplot between IKE and rainfall volume for TCs in the a) East Pacific and b) North Atlantic basin.

Commented [MB4]: 1) What are the uncertainties in the slope and y-intercept? I can tell you how to calculate these – it is easy!
2) Are the plots symmetrical if the axes are flipped? If not, it might seriously alter your interpretation.

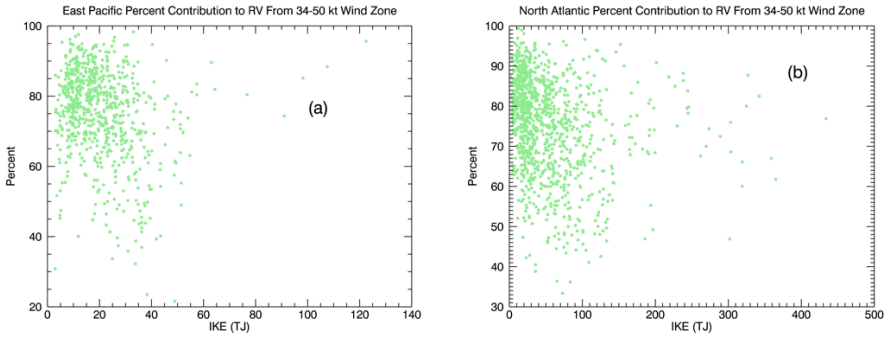

Figure 8: Percent of rainfall volume between 34-50 knot wind radii based on IKE for TC's in the a) East Pacific and b) North Atlantic basin.

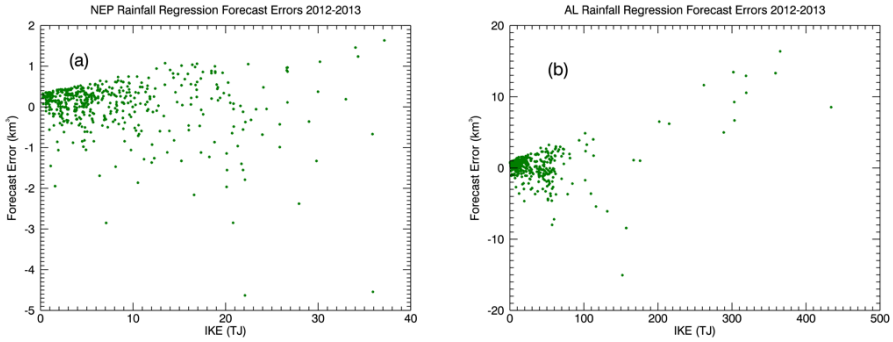

Figure 9: Errors in rainfall prediction for the 2012-2013 seasons, based on a linear regression forecast using 2004-2011 RV and IKE data. a) East Pacific and b) North Atlantic basins.